Phase-retrieval problems in infrared–visible sum-frequency generation spectroscopy by the maximum-entropy method

Pao-Keng Yang and Jung Y. Huang

Institute of Electro-Optical Engineering, Chiao Tung University, Hsinchu, Taiwan, China

Received February 4, 1997; revised manuscript received June 3, 1997

A phase-retrieval procedure based on the maximum-entropy method is applied to infrared–visible sum-frequency generation spectroscopy. Several typical effects on the error phase are also examined with the aid of a known theoretical model. The interference between the resonant and the nonresonant parts changes the behavior of the error phase. Even in some cases when the nonresonant part is complex, the error phase becomes like a step function. This result contradicts the smoothness assumption for the error phase, and the whole phase-retrieval procedure breaks down in these cases. A comparison of the results of phase-retrieval procedures between infrared–visible sum-frequency generation and coherent anti-Stokes Raman scattering spectra is made. Some ideas that worked well in previous analyses of coherent anti-Stokes Raman scattering spectra become inapplicable in the infrared–visible sum-frequency generation spectra in spite of the resemblance of their line shape functions. © 1997 Optical Society of America [S0740-3224(97)01510-5]

1. INTRODUCTION

The maximum-entropy method[1] (MEM) is a useful technique for solving an inverse problem with insufficient information. The result obtained by maximum entropy corresponds to the most probable result in the space of all possible outcomes that satisfy the known information. Such a method has been applied extensively in many disciplines, such as the study of the interior structure of the Earth,[1] image restoration in astronomy,[2] and the phase-extension problem for determining the structures of macromolecular crystals.[3]

Recently there has been some success[4–6] in using the MEM to solve the phase-retrieval problem in nonlinear optical spectroscopy. The maximum-entropy phase-retrieval procedure (MEPRP) is fascinating because it can extract the phase information from an intensity spectrum without knowledge of the theoretical model of the processes concerned. The MEPRP can be regarded as an improved method compared with the Kramers–Kronig relations method[7,8] because the information needed for the MEPRP to improve the accuracy can be found inside the measured range, whereas the Kramers–Kronig relations method needs data that must be extrapolated beyond the spectral range of measurements. In addition, the MEPRP can be applied to cases of harmonic-frequency generation in which the phase reduction from the Kramers–Kronig relations method is shown to be unreliable.[4] The phase-retrieval problem with the MEM can be reduced to estimation of the error phase. In most cases the error phase is a smooth function; polynomial interpolation of few known error-phase points will give a reasonable estimate. For example, in the analysis of the third-order susceptibility spectrum of a poly(dihexylsilane) film, linear interpolation with two known error-phase points will give a satisfactory result,[5] and even in the analysis of coherent anti-Stokes Raman scattering (CARS) spectra, a constant-error-phase assumption can work very well.[6] Although the MEPRP works so well in the cases mentioned above, the basic assumption, the smoothness of the error phase, is so far only illustrated by several examples rather than being strictly justified. It is still questionable why the error phase should be so smooth.

In this paper we apply the MEPRP to infrared–visible sum-frequency generation (IVSFG) spectroscopy,[9] which has proved to be a useful tool for studying surfaces and interfacial phenomena because the process involved is surface specific in the dipole approximation and sensitive to the polar ordering of adsorbed molecules on the surface. IVSFG is a second-order nonlinear-optical process in which two input beams, one at the infrared frequency ω_{IR} and the other at the visible frequency ω_v, interact and generate an output at the sum frequency ω_s in the visible spectrum of light. Here the infrared light source is tunable across some vibrational absorption bands of the adsorbed molecules and the visible light is fixed at some frequency. The spectral line shape of IVSFG resembles that of CARS and can be described by

$$\begin{aligned} I(\omega_s) &\propto |\chi_s^{(2)}(-\omega_s;\ \omega_v,\ \omega_{\mathrm{IR}})|^2 \\ &= |\chi_{\mathrm{NR}}^{(2)} + \chi_{\mathrm{R}}^{(2)}| \\ &= \left| \chi_{\mathrm{NR}}^{(2)} + \sum_q \frac{A_q \gamma_q}{(\omega_q - \omega_{\mathrm{IR}} - i\gamma_q)} \right|^2, \end{aligned} \tag{1}$$

where A_q, ω_q, and γ_q are the resonant strength, the resonant frequency, and the damping constant for the qth vibrational mode and the nonresonant part in Eq. (1) can be complex:

$$\chi_{\mathrm{NR}}^{(2)} = |\chi_{\mathrm{NR}}^{(2)}| \exp(i\theta). \tag{2}$$

0740-3224/97/102443-06$10.00

From the microscopic expression of nonlinear susceptibility, the resonant strength A_q is nonvanishing only if this mode is infrared and Raman active,[10] that is,

$$\left[\frac{\partial \mu_{gg}}{\partial Q_q}\right]_0 \neq 0, \qquad \left[\frac{\partial \alpha_g}{\partial Q_q}\right]_0 \neq 0, \tag{3}$$

where μ_{gg} and α_g are the ground-state dipole momentum and the conventional optical polarizability, respectively, and they can depend on the normal mode coordinate of the qth mode, Q_q. From Eq. (1) the line shape of IVSFG can be described by the interference between the nonresonant part $\chi_{\mathrm{NR}}^{(2)}$ and the resonant part $\chi_{\mathrm{R}}^{(2)}$. Unlike in CARS, which usually has a large nonresonant background, the nonresonant part for IVSFG may be quite small. For example, in IVSFG spectra the nonresonant part of the alkylsilane adsorbed on the fused silica is negligible.[11] Moreover, some IVSFG spectra of diamond films have shown that the nonresonant background $\chi_{\mathrm{NR}}^{(2)}$ can have a relative phase shift ($\theta \neq 0$) with respect to the resonant strength A_q, as the sum frequency is near the resonances of surface electronic states and the ratio of $|A_q|$ to $|\chi_{\mathrm{NR}}^{(2)}|$ can be changed by different coverage.[12] Therefore IVSFG spectra are quite diverse. Before the MEM can be employed as a phase-retrieval technique for IVSFG spectra we should carefully examine whether the error phase is still smooth in every case. In this paper we first theoretically examine several typical effects on the error phase to see whether the smoothness assumption for the error phase is still valid. Owing to the resemblance in the line-shape function between CARS and IVSFG, we are also curious to see whether those ideas that work well in analyzing CARS spectra are still useful in IVSFG.

This paper is organized as follows: In Section 2 we give a brief review of the procedure of phase-retrieval by the MEM. Our results are presented and discussed in Section 3. The conclusion is given in Section 4.

2. PHASE-RETRIEVAL PROCEDURE

The entropy for a power spectrum $S(f)$ in the frequency interval $[f_1, f_2]$ is defined as

$$h \propto \int_{f_1}^{f_2} \log S(f)\mathrm{d}f. \tag{4}$$

In the MEPRP a normalized frequency variable $v = (f - f_1)/(f_2 - f_1)$ is introduced to project the frequency $[f_1, f_2]$ onto $[0, 1]$ to facilitate the calculation. By variational calculus with the Lagrange multiplier method one can find the solution that maximizes the spectral entropy with constraints (known spectral points). The solution for $2M + 1$ spectral points is

$$\hat{S}(v) = \frac{|\beta|^2}{\left|1 + \sum_{k=1}^{M} a_k \exp(i2\pi k v)\right|^2}, \tag{5}$$

where the coefficients a_k and $|\beta|^2$ can be determined from a Toeplitz system:

$$\begin{bmatrix} R(0) & R(-1) & \cdots & R(-M) \\ R(1) & R(0) & \cdots & R(1-M) \\ \vdots & \vdots & \ddots & \vdots \\ R(M) & R(M-1) & \cdots & R(0) \end{bmatrix} \begin{pmatrix} 1 \\ a_1 \\ \vdots \\ a_M \end{pmatrix} = \begin{pmatrix} |\beta|^2 \\ 0 \\ \vdots \\ 0 \end{pmatrix}, \tag{6}$$

where $R(m)$ is the autocorrelation function, which is the Fourier transform of power spectrum $S(v)$:

$$R(m) = \int_0^1 S(v)\exp(-i2\pi m v)\mathrm{d}v. \tag{7}$$

By the same reasoning, the solution of $\chi^{(2)}(v)$ with maximum entropy is

$$\hat{\chi}^{(2)}(v) = \frac{|\beta|\exp[i\phi(v)]}{1 + \sum_{k=1}^{M} a_k \exp(i2\pi k v)}. \tag{8}$$

The solution implies that the process with maximum entropy is a regressive progress. Because coefficients $|\beta|$ and a_k can be obtained by Eq. (6), the error phase $\phi(v)$ is the only quantity in Eq. (8) that cannot be deduced from the power spectrum $S(v)$. The difficulty with the problem of phase-retrieval by the MEM is therefore reduced to find the corresponding error phase $\phi(v)$. There is an one-to-one correspondence between the error phase and the real phase, $\arg[\chi^{(2)}(v)]$. Given a measured phase value at some frequency, we can find the corresponding error phase value at the same frequency. It has been illustrated that $\phi(v)$ is a smooth function, unlike the real-phase behavior, which usually contains step jumps as the frequency is scanned across the resonant frequencies. Usually, linear interpolation of two known error-phase values $\phi(v_1)$ and $\phi(v_2)$, which can be given by two measured real-phase data points, will lead to a good estimate. If more phase values are known, a better estimate can be obtained by polynomial interpolation.

In the MEPRP one can artificially make the error phase more linear by performing a frequency-squeezing procedure.[5,6] For a spectrum measured in a finite range $\omega \in [\omega_1, \omega_2]$, the squeezed spectra, characterized by a squeezing parameter K, are given by

$$|\chi_K^{(2)}(v)| \equiv \begin{cases} |\chi^{(2)}(\omega_1)| & 0 \leq v < \dfrac{K}{2K+1} \\ |\chi^{(2)}(\omega_1 + (\omega_2 - \omega_1)[(2K+1)v - K])| & \dfrac{K}{2K+1} \leq v \leq \dfrac{K+1}{2K+1}. \\ |\chi^{(2)}(\omega_2)| & \dfrac{K+1}{2K+1} < v \leq 1 \end{cases} \quad (9)$$

Thus, choosing the parameter $K > 0$, we transform the original spectrum into a narrower range of normalized frequency. The frequency-squeezing procedure will help to increase the reliability of the linear estimate for the error phase and is usually used in the MEPRP.

3. RESULTS AND DISCUSSIONS

A. Theoretical Analysis of the Error-Phase Behavior in IVSFG Spectroscopy

The effect on the error phase of changing the nonresonant strength is shown in Fig. 1. The filled circles in the figures at the left denote the input theoretical spectrum, and the solid curves are the interpolating curves predicted by the MEM, i.e., Eq. (5). The nonresonant strength is characterized by the value of $|\chi_{\mathrm{NR}}^{(2)}|/|A_q|$, which decreases from top to bottom in Figs. 1(a), 1(b), 1(c), 1(d), and 1(e), with values of 1, 0.5, 0.1, 0.05, and 0.01, respectively. The figures at the right show the corresponding error phases with ($K = 1$) and without ($K = 0$) the frequency-squeezing procedure. Figure 1(a) shows that, for a large nonresonant background, the error phase is really flat except for slight deviation that occurs near the spectral boundaries. Such flat behavior can explain why the constant-error-phase assumption can work successfully in the phase-retrieval procedure for CARS spectra. The frequency-squeezing procedure can improve the result because it can reduce the deviation from a constant value near the boundaries. However, as the nonresonant strength decreases from Fig. 1(a) to Fig. 1(e), the deviation around the boundaries is reduced, and the behavior becomes inclined. This means that the constant-error-phase assumption, which works well in analyzing CARS spectra, will become inapplicable in IVSFG spectra if the nonresonant background becomes negligible. We can see that the error phase is still smooth, and the linear interpolation will give a good estimate. Thus in the cases with negligible nonresonant contributions one must know at least two phase values to get a good estimate of the error phase. We believe that the same problem will occur in the analysis of polarization CARS spectra because in the polarization CARS, with an appropriate polarization arrangement in the detection scheme, the nonresonant background is largely suppressed to yield good sensitivity.[13]

Figure 2 shows the effect on the error phase of changing the nonresonant phase. The nonresonant phase is increasing from Fig. 2(a) to Fig. 2(e). The corresponding nonresonant phase values in Figs. 2(a), 2(b), 2(c), 2(d), and 2(e) are 45°, 90°, 180°, 225°, and 270°, respectively, with the value of $|\chi_{\mathrm{NR}}^{(2)}|/|A_q|$ fixed at 0.6. We can see that the error phase varies considerably from one nonresonant phase value to another. Even the error phases for the spectra of Figs. 2(d) and 2(e) become like step functions. This result conflicts with the assumption of the smoothness for the error phase, and the MEPRP becomes inapplicable in these cases. We also find that the frequency-squeezing procedure cannot lessen the abrupt change in the error phase for Figs. 2(d) and 2(e). Looking at the error phase of Fig. 2(e), we see that the frequency-squeezing procedure causes negligible change in the error phase (the open circles almost overlap the filled circles). The

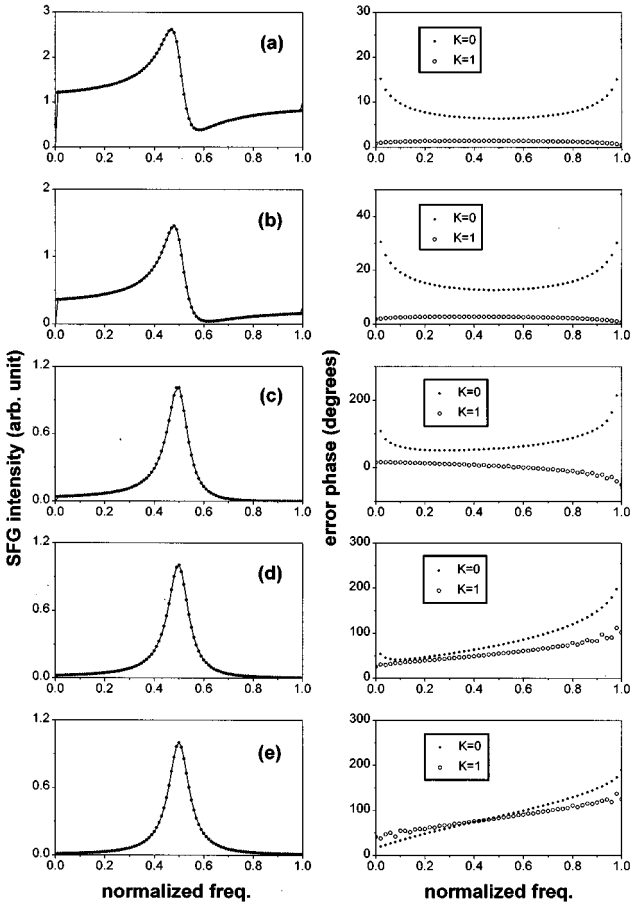

Fig. 1. Effect on the error phase of changing nonresonant strength, illustrated with different $|\chi_{\mathrm{NR}}^{(2)}|/|A_q|$ values. The values of $|\chi_{\mathrm{NR}}^{(2)}|/|A_q|$ are (a) 1, (b) 0.5, (c) 0.1, (d) 0.05, and (e) 0.01. The filled circles in the left-hand figures denote the simulated squared modulus $|\chi^{(2)}|^2$, and the corresponding MEM approximations are shown by the solid curves. The nonresonant strength is decreasing from the top to the bottom. The figures at the right show the corresponding error phases with ($K = 1$) and without ($K = 0$) the frequency-squeezing procedure. SFG, sum-frequency generation.

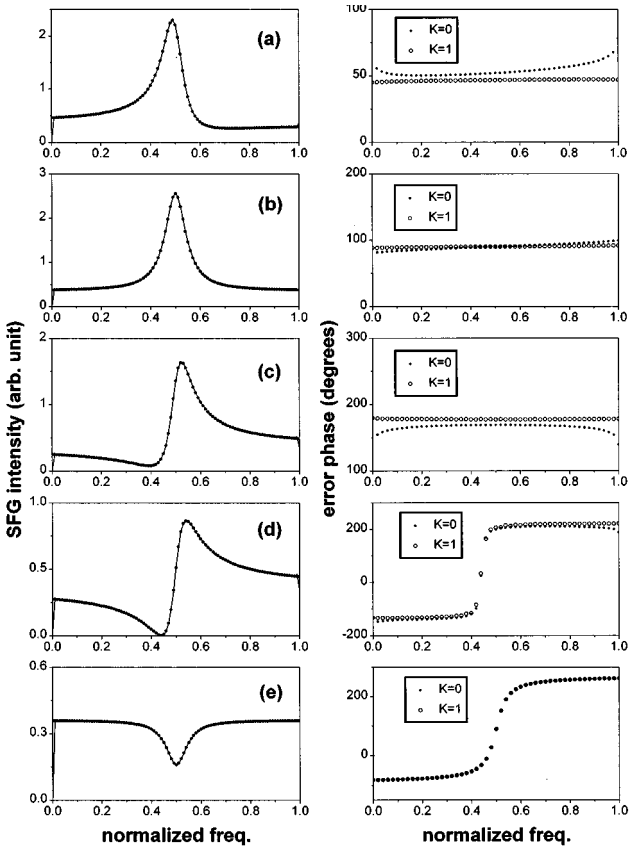

Fig. 2. Effect on the error phase of changing nonresonant phase, illustrated with the values of nonresonant phase of (a) 45°, (b) 90°, (c) 180°, (d) 225°, and (e) 270° and the value of $|\chi^{(2)}_{\mathrm{NR}}|/|A_q|$ fixed at 0.6. The filled circles in the left-hand figures denote the simulated squared modulus $|\chi^{(2)}|^2$, and the corresponding MEM approximations are shown by the solid curves. The nonresonant phase is increasing from the top to the bottom. The figures at the right shows the corresponding error phases with ($K = 1$) and without ($K = 0$) the frequency-squeezing procedure.

diplike spectra shown in Fig. 2(e) have been observed in some experimental IVSFG spectra from the polymer-surfactant adsorbate at the hydrophobic surface.[14]

Figure 3 demonstrates how the error phase is affected as two peaks move toward overlapping. Our result shows that the peaks' overlapping does not have a significant effect on the error-phase behavior. This result is interesting because our previous results illustrated that the interference between a resonant peak and the constant nonresonant background does change the error-phase behavior; here we show that the interference between two resonant peaks has a negligible effect on the error phase.

In the expression of Eq. (1), the effect of vibrational dephasing and relaxation on the linewidth is incorporated through γ_q, and we have not taken the inhomogeneous broadening of the resonant frequencies into account yet. However, some spectra obtained from silver[15] have shown that the inclusion of inhomogeneous broadening did improve the fit around the resonant frequencies. With the inclusion of inhomogeneous broadening, the nonlinear-optical phenomenon can be described by an effective nonlinear-optical susceptibility:

$$\chi^{(2)}_{s,\mathrm{eff}}(\omega_{\mathrm{IR}},\ \omega_q^0) = \int_{-\infty}^{\infty} \chi^{(2)}_s(\omega_{\mathrm{IR}},\ \omega_q)\ \frac{1}{\sqrt{2\pi}\sigma} \times \exp\left[-\frac{1}{2\sigma^2}(\omega_q - \omega_q^0)^2\right] \mathrm{d}\omega_q . \tag{10}$$

Here we assume that the vibrational frequencies ω_q have a Gaussian distribution about a central frequency ω_q^0, with standard deviation σ. In Fig. 4 we show the inhomogeneous broadening effect on the error phase for an isolated spectral peak. The values of σ/γ used in Figs. 4(a), 4(b), 4(c), and 4(d) are chosen to be 0.1, 0.2, 1, and 2, respectively. According to our result, the inhomogeneous broadening seems not to influence the error phase. For different σ/γ values the error phase remains almost unchanged, even in the cases when the spectral response has been considerably broadened, as shown in Fig. 4(d). Thus we conclude that inhomogeneous broadening plays a minor role in the determination of an error phase and that it will not affect the phase-retrieval procedure.

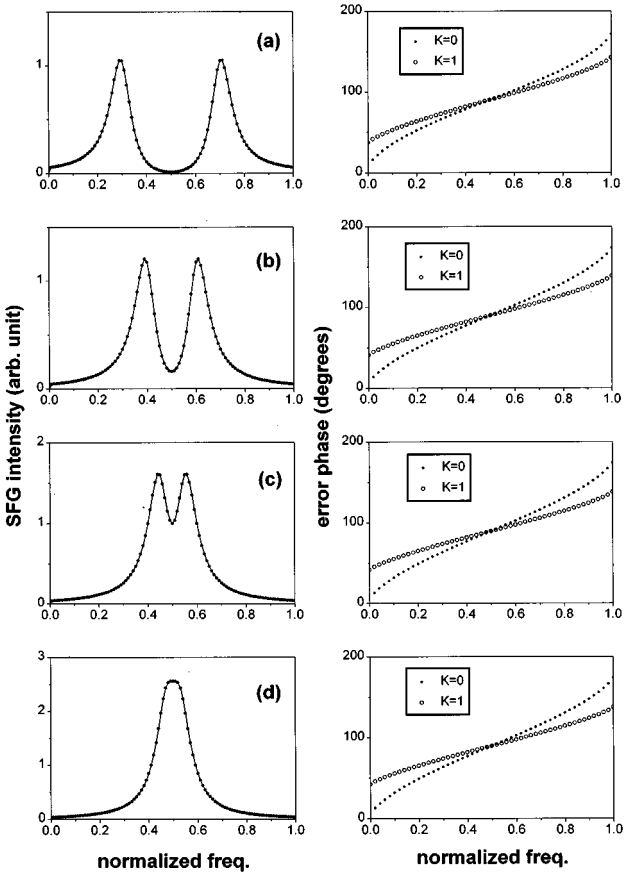

Fig. 3. Effect of peak overlapping on the error phase. The filled circles in the left-hand figures denote the simulated squared modulus $|\chi^{(2)}|^2$, and the corresponding MEM approximations are shown by the solid curves. The two spectral peaks are getting progressively closer from (a) to (d), and the corresponding error phases with ($K = 1$) and without ($K = 0$) the frequency-squeezing procedure are shown at the right.

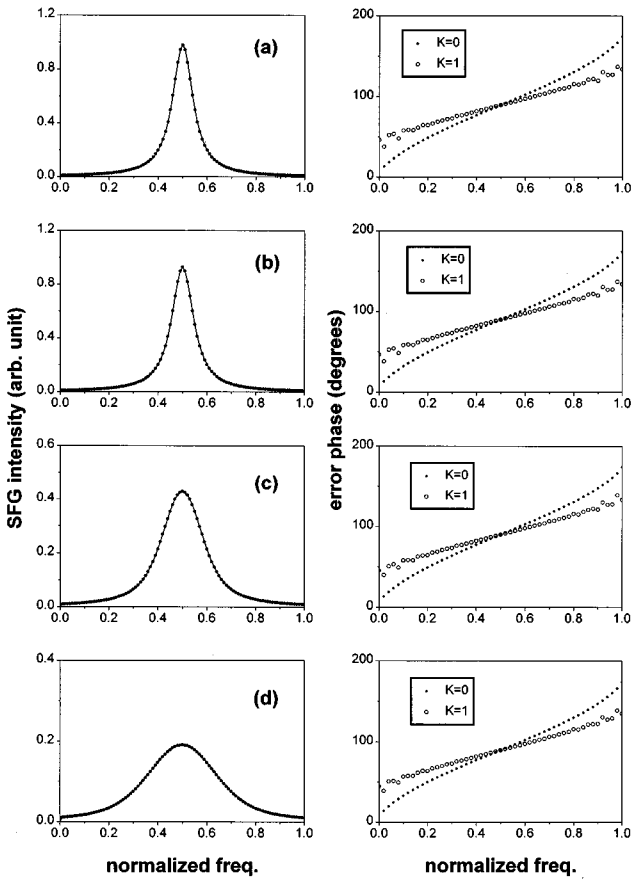

Fig. 4. Effect on the error phase of inhomogeneous broadening for an isolated spectral peak. The filled circles in the left-hand figures denote the simulated squared modulus $|\chi^{(2)}|^2$, and the corresponding MEM approximations are shown by the solid curves. The values of σ/γ are 0.1, 0.2, 1, and 2 in (a), (b), (c), and (d), respectively. The figures at the right show the corresponding error phases with ($K = 1$) and without ($K = 0$) the frequency-squeezing procedure.

B. Analysis of an Experimental Result

Now we apply the MEPRP to an experimental spectrum from a compact monolayer of pentadecanoic acid with some available phase data.[16,17] We carried out the phase measurement for IVSFG by analyzing the interference patterns from quartz and a monolayer sample. The filled squares in Fig. 5(a) denote the measured IVSFG spectrum versus ω_{IR} for the symmetric CH_3 stretch of pentadecanoic molecules. The measured phase data are given by the filled squares with error bars in Figs. 5(b)–5(d). Because the measured spectral data points in Fig. 5(a) are few, we apply the cubic spline fit to interpolate the raw data to get more data points. The MEM estimate for the spectrum is represented by the solid curve in Fig. 5(a). We estimate the error phase in Fig. 5(b) by a constant value, which is the error-phase value that corresponds to the measured phase indicated by the arrow. The phase predicted from the MEPRP is shown by the solid curve. We find that the constant-error-phase assumption, which works well in CARS, does not predict other measured phase points well. In Figs. 5(c) and 5(d) the error phase is estimated by the linear interpolation of two error phase points, which are obtained from two measured phase points indicated by the arrows. Figure 5(c) also shows that the MEPRP may not well predict the phase far away from the two points used for linear interpolation if the points are too close to each other. From the result in Fig. 5(d) we can see that the MEPRP does predict phase well by the linear interpolation of the error phase. This result is consistent with our previous theoretical analysis of the effect of nonresonant strength on the error phase, in which we found that the constant-error-phase assumption will break down as the nonresonant background becomes negligible and that a linear interpolation can give a good estimate of the error phase. Comparing Fig. 5(c) with Fig. 5(d), we also find that the intrapolation will give a better estimate of error phase than will extrapolation.

C. Problems with Phase Retrieval by Some *a priori* Information for IVSFG Spectra

According to the phase-retrieval procedure in CARS, the MEPRP can be achieved only by a single piece of *a priori* information (i.e., without measuring any phase point experimentally) about the complex function $\chi^{(3)}$. One can obtain such information by adjusting the constant value of the error phase such that the position of a maximum of the imaginary part of $\chi^{(3)}$ merges with that of the local resonant frequency. The above idea really gives a good prediction of the real and the imaginary parts of $\chi^{(3)}$ in CARS, except that some deviation occurs in the imaginary part near the boundaries. It was also shown that the deviation near the boundaries can be reduced by a frequency-squeezing procedure.

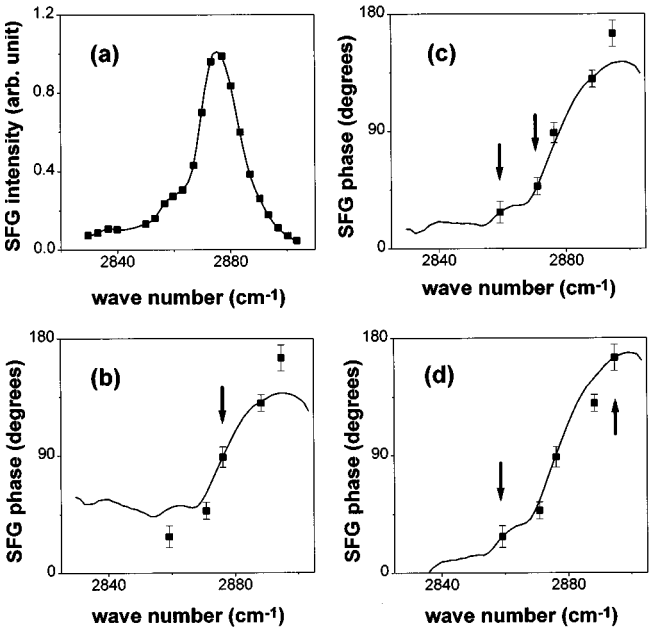

Fig. 5. (a) Measured IVSFG spectrum (filled squares) of the CH_3 symmetric stretch of the pentadecanoic acid monolayer on the water surface and its MEM interpolation (solid curve). (b)–(d) Measured phase values (filled squares) and the estimated phases (solid curves) from the MEPRP. The error phase in (b) is estimated by a constant value that is the error-phase value corresponding to the measured phase value indicated by an arrow. The error phases in (c) and (d) are estimated by linear interpolation of two error-phase values corresponding to the measured phase values shown by the arrows.

From our previous theoretical analysis of error-phase behavior, for the cases with negligible nonresonant background, at least two pieces of *a priori* information must be known to give a good estimate of the error phase. In such cases we can first assume that the error phase is a linear function, $\phi(v) = \phi_0 + \phi_1 v$, and then solve the two unknown constants, ϕ_0 and ϕ_1, by applying the same criteria as used in CARS to two peaks in the spectra; that is,

$$\frac{\partial}{\partial v}\{\mathrm{Im}[\chi(v)]\}_{v=v_{R1}} = 0,$$

$$\frac{\partial}{\partial v}\{\mathrm{Im}[\chi(v)]\}_{v=v_{R2}} = 0. \tag{11}$$

Therefore we can hope to apply the MEPRP to IVSFG spectra without measuring any phase values. However, because the IVSFG signal is sensitive to the polar ordering of the adsorbed molecules on the surface, the signal will be vanishing for samples composed of randomly oriented molecules if there is no nonresonant background. For some ordered monolayer, if we reverse all polar orientation of all adsorbed molecules, the second-order nonlinear susceptibility $\chi^{(2)}$ for the system before and after the reversing operation is applied will have opposite sign but the same modulus. Thus two systems with reversed molecular orientation will result in the same power spectrum, so we cannot distinguish one polar orientation from its reversed orientation purely from the power spectrum. That is, one cannot use the phase obtained from the MEPRP by some *a priori* information to determine the absolute polar orientation of the adsorbed molecules. It is easy to see that the failure in determining the absolute polar orientation can be regarded as a 180° ambiguity in the error phase or in the real phase, which one can solve only by carrying out the absolute phase measurement[17] or by a circular-dichroism type experiment if the adsorbed molecules are chiral.[18]

4. CONCLUSION

We have used the MEM to study the phase-retrieval problem for IVSFG spectra. Several typical effects on error-phase behavior were examined with the known theoretical model. We found that the error phase is not influenced by the overlapping of the peaks and inhomogeneous broadening effects but can be affected by changes in the nonresonant amplitude and the nonresonant phase. For spectra with small nonresonant backgrounds, at least two pieces of phase information are needed to yield a good estimate of the error phase; we verified this fact by analysis of an experimental result. In some cases when the nonresonant part is complex, the error phase will contain a step-jump behavior. Such a result conflicts with the smoothness assumption for the error phase and makes the MEPRP inapplicable. We also discussed the problem of phase retrieval by some *a priori* information. We found that there is an ambiguity in the final result if only the intensity spectra are known at first. That is, one cannot use the phase obtained by some *a priori* information to determine the absolute polar orientation of the adsorbed molecules.

ACKNOWLEDGMENT

We appreciate financial support by the National Science Council of the Republic of China under grant NSC86-2112-M009-018.

Address any correspondence to P.-K. Yang. E-mail: u8224809@cc.nctu.edu.tw.

REFERENCES

1. R. M. Bevensee, *Maximum Entropy Solutions to Scientific Problems* (Prentice-Hall, Englewood Cliffs, N.J., 1993).
2. N. L. Bonavito, J. E. Dorband, and T. Busse, "Maximum entropy restoration of blurred and oversaturated Hubble telescope imagery," Appl. Opt. **32**, 5768–5774 (1993).
3. E. Prince, "Construction of maximum-entropy density maps, and their use in phase determination and extension," Acta Crystallogr. **49**, 61–66 (1993).
4. E. M. Vartiainen and K.-E. Peiponen, "Meromorphic degenerate nonlinear susceptibility: phase retrieval from the amplitude spectrum," Phys. Rev. B **50**, 1941–1944 (1994).
5. E. M. Vartiainen, K.-E. Peiponen, H. Kishida, and T. Koda, "Phase retrieval in nonlinear optical spectroscopy by the maximum-entropy method: an application to the $|\chi^{(3)}|$ spectra of polysilane," J. Opt. Soc. Am. B **13**, 2106–2114 (1996).
6. E. M. Vartiainen, "Phase retrieval approach for coherent anti-Stokes Raman scattering spectrum analysis," J. Opt. Soc. Am. B **9**, 1209–1214 (1992).
7. F. L. Ridener and R. H. Good, "Dispersion relations for nonlinear systems of arbitrary degree," Phys. Rev. B **11**, 2768–2770 (1975).
8. H. Kishida, T. Hasegawa, Y. Iwasa, T. Koda, and Y. Tokura, "Dispersion relation in the third-order electric susceptibility for polysilane film," Phys. Rev. Lett. **14**, 3724–3727 (1993).
9. J. Y. Huang and Y. R. Shen, "Sum-frequency generation as a surface probe," in *Laser Spectroscopy and Photochemistry on Metal Surfaces*, H. L. Dai and W. Ho, eds. (World Scientific, Singapore, 1995), Vol. 1, pp. 5–53.
10. S. H. Lin and A. A. Villaeys, "Theoretical description of steady-state sum-frequency generation in molecular adsorbates," Phys. Rev. A **50**, 5134–5144 (1994).
11. P. Guyot-Sionnest, R. Superfine, J. H. Hunt, and Y. R. Shen, "Vibrational spectroscopy of a silane monolayer at air/solid and liquid/solid interfaces using sum-frequency generation," Chem. Phys. Lett. **144**, 1–5 (1988).
12. R. P. Chin, J. Y. Huang, Y. R. Shen, T. J. Chuang, H. Seki, and M. Buck, "Vibrational spectra of hydrogen on diamond $C(111)-(1\times 1)$," Phys. Rev. B **45**, 1522–1524 (1992).
13. Y. R. Shen, *The Principles of Nonlinear Optics* (Wiley, New York, 1984), pp. 272–275.
14. D. C. Duffy, P. B. Davies, and A. M. Creeth, "Polymer-surfactant aggregates at a hydrophobic surface studied using sum-frequency vibrational spectroscopy," Langmuir **11**, 2931–2937 (1995).
15. T. H. Ong, P. B. Davies, and C. D. Bain, "Sum-frequency spectroscopy of alkoxy-terminated alkanethiols in contact with liquid," Langmuir **9**, 1836–1845 (1993).
16. R. Superfine, J. Y. Huang, and Y. R. Shen, "Phase measurement for surface infrared–visible sum-frequency generation," Opt. Lett. **15**, 1276–1278 (1990).
17. R. Superfine, J. Y. Huang, and Y. R. Shen, "Experimental determination of the sign of molecular dipole derivatives: an infrared–visible sum frequency generation absolute phase measurement study," Chem. Phys. Lett. **172**, 303–306 (1990).
18. J. D. Byers, H. I. Yee, T. Petralli-Mallow, and J. M. Hicks, "Second-harmonic generation circular-dichroism spectroscopy from chiral monolayers," Phys. Rev. B **49**, 14,643–14,647 (1994).